



1 **Historical variation in normalized difference vegetation index**
2 **compared with soil moisture at a taiga forest ecosystem in**
3 **northeastern Siberia**

4 Aleksandr Nogovitsyn¹, Ruslan Shakhmatov^{1,2}, Tomoki Morozumi³, Shunsuke Tei^{4,5}, Yumiko
5 Miyamoto^{4,6}, Nagai Shin⁷, Trofim C. Maximov⁸ and Atsuko Sugimoto⁴

6 ¹Graduate School of Environmental Science, Hokkaido University, Sapporo, 060-0817, Japan

7 ²Slavic-Eurasian Research Center, Hokkaido University, Sapporo, 060-0809, Japan

8 ³National Institute for Environmental Studies, Tsukuba, 305-8506, Japan

9 ⁴Arctic Research Center, Hokkaido University, Sapporo, 001-0021, Japan

10 ⁵Forestry and Forest Products Research Institute, Tsukuba, 305-8687, Japan

11 ⁶Faculty of Agriculture, Shinshu University, Kamiina, 399-4598, Japan

12 ⁷Research Institute for Global Change, Japan Agency for Marine-Earth Science and Technology, Yokohama, 236-0001, Japan

13 ⁸Institute for Biological Problems of Cryolithozone, Siberian Branch of the Russian Academy of Sciences, Yakutsk, 677000,
14 Russia

15 *Correspondence to:* Atsuko Sugimoto (sugimoto@star.dti2.ne.jp)

16 **Abstract.** The taiga ecosystem in northeastern Siberia, a nitrogen-limited ecosystem on permafrost with a dry climate, changed
17 during the extreme wet event in 2007. We investigated the normalized difference vegetation index (NDVI) as a satellite-derived
18 proxy of needle production and compared it with ecosystem parameters such as soil moisture water equivalent (SWE), foliar
19 C/N ratio, $\delta^{13}\text{C}$ and $\delta^{15}\text{N}$, and ring width index (RWI) at the Spasskaya Pad Experimental Forest Station in Russia for the period
20 from 1999 to 2019. Historical variations in NDVI showed a large difference between typical larch forest (unaffected) and the
21 sites affected by the extreme wet event in 2007 because of high tree mortality at affected sites under extremely high SWE and
22 waterlogging, resulting in a decrease in NDVI. Before 2007, the NDVI in a typical larch forest showed a positive correlation
23 with SWE and a negative correlation with foliar C/N. These results indicate that not only the water availability (high SWE) in
24 the previous summer and current June but also the soil N availability increased needle production. NDVI was also positively
25 correlated with RWI, resulting from similar factors controlling them. However, after the wet event, NDVI was negatively
26 correlated with SWE, while NDVI showed a negative correlation with foliar C/N. These results indicate that after the wet event,
27 high soil moisture availability decreased needle production, which may have resulted from lower N availability. Needle $\delta^{15}\text{N}$
28 was positively correlated with NDVI before 2007, but after the wet event, needle $\delta^{15}\text{N}$ decreased. This result suggests damage
29 to roots and/or changes in soil N dynamics due to extremely high soil moisture.

30 **1 Introduction**

31 Boreal forests in northern regions of North America and Eurasia, including islands, occupy a large forest area, approximately



32 27 % (Fao, 2020). Under conditions of increasing atmospheric CO₂ concentrations (e.g. Friedlingstein et al., 2022), the role of
33 taiga and other terrestrial ecosystems as carbon sinks becomes more important. Among the taiga areas, Alaska, Canada, and
34 Siberia are distinguished by permafrost, which is one of the main components of the global carbon cycle. Siberian taiga is
35 covered with coniferous trees, mainly larches, which grow under severe conditions, such as continental climate, that is, cold
36 winters, hot summers, low precipitation (Archibold, 1995), and limited nitrogen availability (Popova et al., 2013; Kajimoto et
37 al., 1999). Permafrost and seasonal ice are important sources of water for larches during drought (Sugimoto et al., 2003;
38 Sugimoto et al., 2002). These conditions make this ecosystem vulnerable to environmental changes. Under warming,
39 permafrost may decline, which can trigger large amounts of carbon emissions (Schuur et al., 2015) and change the ecosystem.
40 In eastern Siberia, the role of the taiga ecosystem and its responses to climate change have been studied at the Spasskaya Pad
41 Forest Station near Yakutsk. This larch forest is a net CO₂ sink; however, quantitative estimations of the flux from tower
42 measurements and various models differ (Takata et al., 2017). Over the past few decades, tree ring growth has decreased, and
43 according to the tree-ring width index (RWI)-based statistical model, the radial growth of trees is expected to have a negative
44 trend because of high temperature-induced drought (Tei et al., 2017). On the other hand, precipitation extremes, which are
45 predicted to be more intensive and frequent (Douville et al., 2021), can also negatively affect the forest. Larch roots, which
46 usually take up water from seasonal ice in the active layer (above the permafrost) under dry conditions, can adapt to wet
47 conditions by decreasing vertical distribution (Takenaka et al., 2016). However, the extreme wet event in 2007, when soil
48 moisture was the highest in the past century (Tei et al., 2013), was fatal for many trees in the forest, especially in depressions
49 (Iijima et al., 2014; Ohta et al., 2014). In addition to high tree mortality, affected sites are distinguished by a secondary
50 succession of the understory and floor vegetation communities to water-resistant species (Ohta et al., 2014). It was suggested
51 that such sites in the forest generally emit methane, which makes the ecosystem a net CH₄ source according to estimations of
52 open-path eddy covariance measurements (Nakai et al., 2020). The wet event was caused by continuous heavy precipitation,
53 including extremely large snowfall. Snow manipulation experiments in the forest showed the influence of interannual variation
54 in winter precipitation on the phenology and production of soil inorganic nitrogen (Shakhmatov et al., 2022). After the extreme
55 moist conditions formed in 2005–2009, eddy-covariance flux measurements showed no significant trends in CO₂ exchange at
56 the ecosystem scale, but the contribution of understory and floor vegetations to CO₂ fluxes increased with biomass, whereas
57 that of overstory larch decreased (Kotani et al., 2019). The high mortality of larches in 2007 could have been caused by two
58 consecutive extreme events—drought and wetness (Tei et al., 2019a). Severe drought and moist conditions in the forest lead to
59 changes in the normalized difference vegetation index (NDVI) (Tei et al., 2019b; Nagano et al., 2022), which is considered a
60 proxy of vegetation productivity. However, gross primary production (GPP) was found to be more related to the larch tree RWI
61 in 2004–2014, but not to NDVI, because of changes in the understory and floor vegetation composition (Tei et al., 2019b).
62 Based on an investigation of spatial variations in NDVI and foliar parameters in 2018, Nogovitsyn et al. (2022) found that



63 affected sites with lower NDVI due to a smaller number of living mature trees showed higher nitrogen and light availabilities
64 (higher foliar C/N and $\delta^{13}\text{C}$, respectively) due to low competition for resources. These favorable conditions can contribute to
65 further succession. Although many studies have been conducted in eastern Siberia, no study has focused on the relationships
66 between historical NDVI and foliar parameters in this region.

67 The taiga ecosystem in eastern Siberia is one of the most important biomes in the world and is vulnerable to climate change.
68 The purpose of this study was to understand how the larch forest in this region changed and what factors impacted the changes
69 over the past two decades. We investigated historical variations in satellite-derived NDVI and field-observed parameters, such
70 as the RWI, soil moisture, needle $\delta^{13}\text{C}$, $\delta^{15}\text{N}$, C/N, air temperature, and precipitation from 1998 to 2019.

71 **2 Materials and Methods**

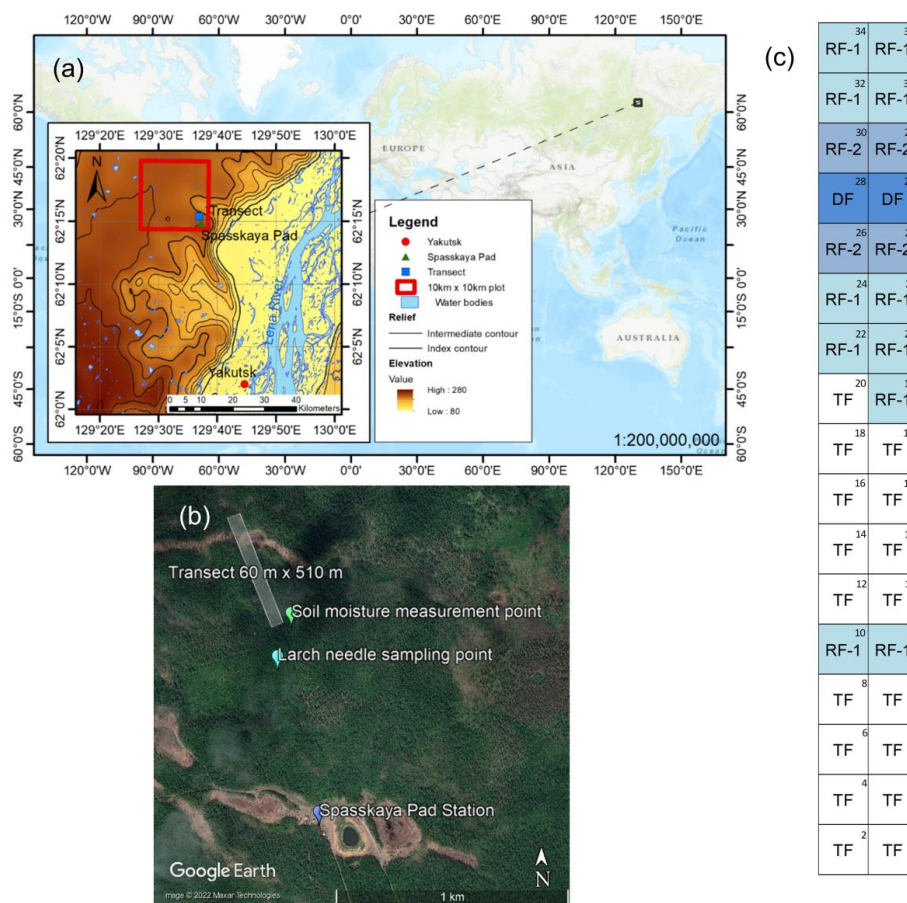
72 **2.1 Study site**

73 The study was conducted in the Spasskaya Pad Experimental Forest (62°15'18"N, 129°37'08"E, alt. 220 m a.s.l.), Institute of
74 Biological Problems of Cryolithozone, Siberian Branch of the Russian Academy of Sciences (IBPC SB RAS), near Yakutsk,
75 Russia (Fig. 1a). The region in Eastern Siberia is established on continuous permafrost and has a continental climate (dry
76 climate) with an extremely high annual temperature range. During the observation period from 1991 to 2020 at Yakutsk, the
77 average annual precipitation was 233 mm, and the average monthly temperature ranged from -37°C to +20 °C in cold January
78 and warm July, respectively. The overstory (forest canopy) consists of deciduous species, dominant coniferous larch (*Larix*
79 *cajanderi*) (Abaimov et al., 1998) mixed with broadleaved birch (*Betula pendula*), and the understory includes small shrubs,
80 such as evergreen cowberry (*Vaccinium vitis-idaea*) and deciduous bearberry (*Arctous alpina*), and other grasses.

81 During the period from 2005 to 2007 (water years, from October to September), there was a large amount of precipitation (307
82 \pm 29 mm) continuously, which caused a significant increase in soil moisture (Sugimoto, 2019) and even waterlogging.
83 Consequently, an extreme wet event occurred in 2007, which damaged larch forests, resulting in high tree mortality and a
84 change in the composition of understory vegetation to moisture-tolerant grasses and shrubs in some areas, especially in
85 depressions (Iijima et al., 2014; Iwasaki et al., 2010; Ohta et al., 2014). In the summer of 2018, we set a 60 m \times 510 m transect,
86 which included areas unaffected and affected by the extreme wet event (Fig. 1a, b). The plots were divided into 30 \times 30 m plots
87 (34 plots in total). Using these plots, we observed spatial variation in NDVI (Nogovitsyn et al., 2022). In this study, we visually
88 classified the forest conditions based on photographs. Four forest types were identified along the transect (Fig. 1c): typical
89 mature (TF; number of plots in the transect, $n = 17$), regenerating-1 (RF-1; $n = 11$), regenerating-2 (RF-2; $n = 4$), and damaged
90 (DF; $n = 2$) forests. The first TF showed no visible damage from the extreme wet event. The plots discerned as regenerating
91 forests RF-1, had many dead mature larches and formed forest gaps in the overstory where there were a large number of young
92 larches (seedlings and saplings with a height of up to 3 m) and shrubs. Damaged forests, DF, where all mature trees died, was



93 predominantly covered by moisture-tolerant grasses, and had much smaller numbers of young larches than in RF-1. The DF
 94 plots were located on a depression in a trough-and-mound topography, and some patches of the DF plots were flooded.
 95 Regenerating forests RF-2 had moderate forest conditions between RF-1 and DF.



96
 97 **Figure 1.** (a) Location of the Spasskaya Pad Station (62°15'18"N, 129°37'08"E) and the study transect near Yakutsk in the
 98 topographic map zoomed from a global map. (b) Detailed view of the study area in the Spasskaya Pad Forest: locations of the
 99 station, 60 m x 510 m transect, and points of soil moisture measurement and larch needle sampling for $\delta^{13}\text{C}$, $\delta^{15}\text{N}$, and C/N.
 100 (c) Scheme of the transect with a total of 34 plots, which were divided into four forest types based on the level of forest damage
 101 (Nogoviteyn et al., 2022): typical forests (TF), two types of regenerating forests (RF-1 and RF-2), and damaged forests (DF).

102 2.2 NDVI

103 The raster normalized difference vegetation index (NDVI) was computed based on the Landsat Collection-1 Level-2 image
 104 products with a spatial resolution of 30 m using QGIS software (v. 3.2.2-Bonn):

105
$$\text{NDVI} = (\text{NIR} - \text{R}) / (\text{NIR} + \text{R}),$$



106 where NIR and R are the near-infrared and red surface reflectance bands of the product, respectively. The image products
107 georeferenced to the WGS-84 UTM 52N coordinate system were selected according to the location of the study transect. The
108 NDVI value was extracted for each transect plot using the zonal statistical function. The transect plots, which consist of pixels
109 not attributed to quality pixels (clear terrain, low-confidence cloud, and low-confidence cirrus) in the quality assessment bit
110 index band according to Landsat Surface Reflectance product guides, were excluded from the analysis.

111 To investigate the historical variation in NDVI, we considered the seasonal maximum of the mean NDVI of the transect for
112 the long-time period from 1999 to 2019. The longest time-series data available for the study area has been obtained by the
113 Landsat 7 satellite with the Enhanced Thematic Mapper Plus (ETM+) image sensor since 1999. However, its sparse temporal
114 resolution (16 days) and scan-line corrector failure in 2003 forced the consideration of additional data from other satellites,
115 such as Landsat 5 Thematic Mapper (TM) (available until 2011) and Landsat 8 Operational Land Imager (OLI) (available since
116 2013). Because the last two have different sensors in contrast to Landsat 7, NDVI values calculated from the TM and OLI
117 images were converted to ETM+ using the linear equations:

$$118 \quad \text{NDVI}_{\text{ETM+}} = 1.037 \cdot \text{NDVI}_{\text{TM}},$$

$$119 \quad \text{NDVI}_{\text{ETM+}} = 0.9589 \cdot \text{NDVI}_{\text{OLI}} + 0.0029$$

120 developed by Ju and Masek (2016) and Roy et al. (2016), respectively, for boreal forests. For each year, a paired sample *t*-test
121 was applied to determine the difference between the mean NDVI of the transect on the observation days. In the case of
122 statistically insignificant differences among observation days, we selected the day with the highest number of quality pixels.

123 To verify the historical variation in NDVI of the transect, a larger area, 10 km × 10 km (hereafter, the 10-km plot), including
124 the Spasskaya Pad Forest, was used for comparison with the transect (the center of the 10-km plot was located at 62°17'4"N,
125 129°32'44"E; Fig. 1a). For each observation day, the mean NDVI of the 10-km plot was calculated using only quality pixels
126 using ENVI 5.1 (L3Harris Technologies, USA). For each year, the seasonal maximum NDVI of the 10-km plot was determined
127 as the highest mean NDVI among observation days, on which the number of quality pixels were more than 50 % (total, 111,556
128 pixels). The seasonal maximums of the transect and 10-km plot showed the same day for about three-quarters of the study
129 period (15 years among 21) and showed a different day in six years (Table S1): 2006 (7 August and 29 July), 2007 (1 and 25
130 July), 2010 (1 and 15 July), 2011 (5 and 12 August), 2015 (23 and 31 July), and 2019 (1 and 9 July). The averaged NDVI
131 values of the 10-km plot, transect, and each forest type (TF, RF-1, RF-2, and DF) in the transect are shown in Fig. 2a and 2b.

132 **2.3 Ecosystem and climate parameters**

133 Several ecosystem parameters have been observed since 1998 in typical forests. To monitor the physiological response of larch
134 to environmental changes, the $\delta^{13}\text{C}$ (‰), $\delta^{15}\text{N}$ (‰), and C/N of larch needles have been observed since 1999, except in 2012
135 (0.2 km south of the transect; Fig. 1b). In mid-August every year, four to eight young larch trees close to each other were
136 sampled, and the average values of $\delta^{13}\text{C}$ (‰), $\delta^{15}\text{N}$ (‰), and C/N of these samples were used. The details of the average



137 calculations are shown in Fig. S1 and S2. In 2015, there were no data on the $\delta^{15}\text{N}$ and N content.
138 For more than 100 years, until 2016, larch ring-width index (RWI) was estimated by detrending and standardizing the raw
139 time-series width data obtained from the collected paired cores (Tei et al., 2019b). The RWI data used for analysis are shown
140 in Table S2.
141 Soil moisture was measured using time-domain reflectometry (TDR), and the soil moisture water equivalent (SWE; the amount
142 of liquid water contained within the soil layer, mm) in the 0–60 cm soil layer was obtained for 1998–2019 in June, July, and
143 August using the method described by Sugimoto et al. (2003) (near the transect; Fig. 1b). There were no data for June of 2002
144 and 2011 and August of 2003. The details of the intra- and inter-annual variations in SWE are shown in Fig. S3.
145 Among the climate variables, summer air temperature and precipitation datasets recorded by the meteorological station at
146 Yakutsk (62.02° N, 129.72° E) were obtained from the All-Russia Research Institute of Hydrometeorological Information -
147 World Data Centre (RIHMI-WDC) website (<http://aisori-m.meteo.ru/>).

148 **2.4 Statistical analysis**

149 All statistical analyses were carried out using R statistics v.4.1.3 (R Core Team). Relationships between datasets were
150 investigated using a simple linear regression model (function “lm”) and a Pearson correlation test (“cor.test”). Trends of NDVI
151 change in 1999–2019 were estimated using the Mann–Kendall test (package “trend”, function “mk.test”). Differences in NDVI
152 between the two groups (forest types) were determined using two parametric unpaired two-sample tests, classical Student’s
153 and Welch’s *t*-tests, and one non-parametric Wilcoxon rank-sum test. The criteria for applying a particular test were the data
154 distribution type (normal or non-normal) and the relation of the data variances to each other (equal or unequal): Student’s *t*-
155 test, both datasets have “normal” distributions and “equal” variances; Welch’s *t*-test, “normal”, “unequal”; and Wilcoxon rank-
156 sum test, “non-normal”, “unequal”. Data normality and variance equality were checked using the Shapiro–Wilk test and *F*-test.
157 The results of the statistical tests are shown in the Supplemental (Table S3–S10). The models and tests described by levels of
158 statistical significance (*p*-values) less than 0.05 and 0.1 were considered to be “significant” and “moderately significant”,
159 respectively.

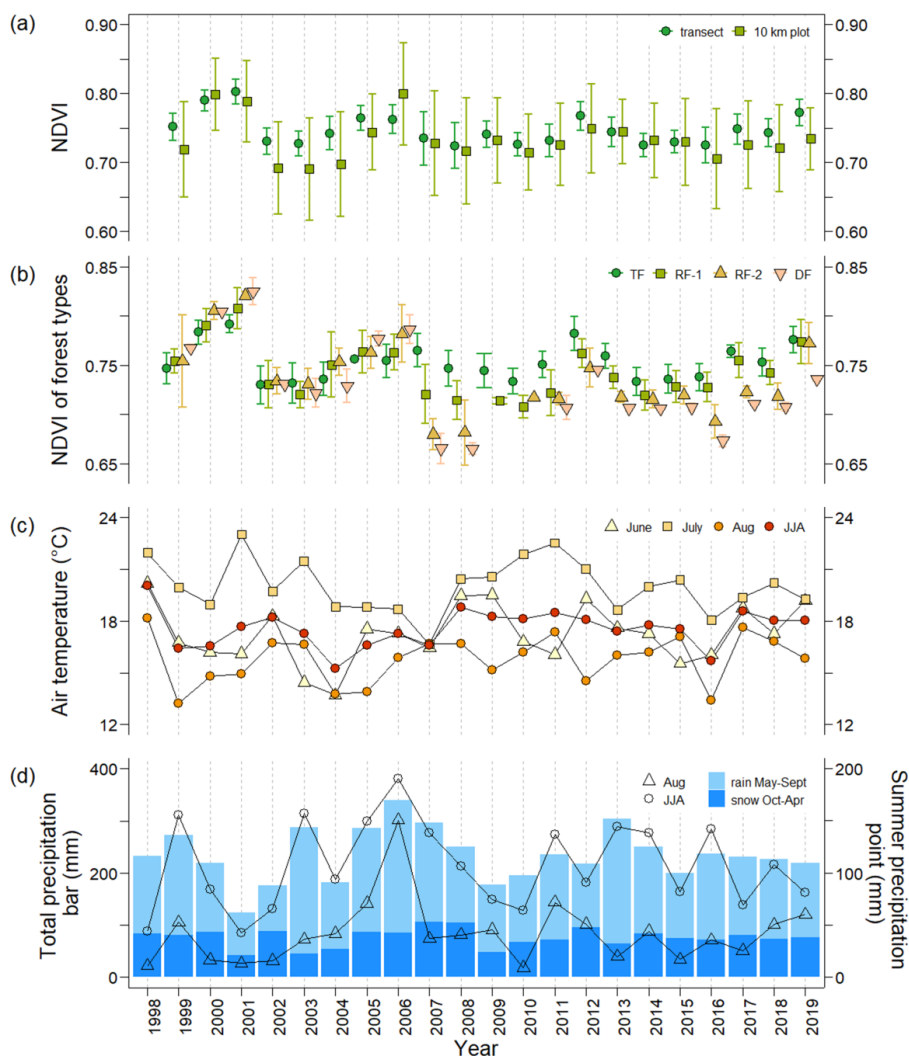
160 **3 Results**

161 **3.1 Year-to-year variation of seasonal maximum NDVI**

162 Fig. 2a shows the historical variation in the seasonal maximum NDVI of the TF and the 10-km plot from 1999 to 2019. Both
163 NDVI time series varied similarly. The seasonal maximum of each year was observed from 25 June to 13 August, except for
164 1999 (shown in Table S2). The maximum transect NDVI in 1999 was observed on 27 August (0.75 ± 0.02 , $n = 34$) because the
165 Landsat data in 1999 were limited to the latter half of August. The mean seasonal maximum NDVI for the transect varied



166 between 0.72 and 0.80. During the period from 1999 to 2001, the NDVI of the transect was high from 0.75 ± 0.02 ($n = 34$) to
 167 0.80 ± 0.02 ($n = 34$) (Fig. 2a), but in 2002 and 2003, the NDVI was much lower (0.73 ± 0.02 , $n = 34$) than that in 2001. From
 168 2003 to 2006, NDVI again increased from 0.73 ± 0.02 ($n = 34$) to 0.76 ± 0.02 ($n = 34$). During the wet event in 2007–2008,
 169 the NDVI decreased to 0.73 ± 0.04 ($n = 34$). After 2009, NDVI was higher than that in 2008 (0.72 ± 0.03 , $n = 34$), except in
 170 2016 (0.72 ± 0.03 , $n = 31$).



171
 172 **Figure 2.** The temporal variations from 1999 to 2019 in (a) seasonal maximum NDVI averaged for the plots in the transect
 173 and the representative 10km x 10km forest plot calculated from available Landsat 5, 7, 8 images; (b) NDVI of four forest types,
 174 typical mature forest (TF), regenerating forests (RF-1 and FR-2), and damaged forest (DF); (c) mean air temperature in June,
 175 July, August and whole summer period JJA (June-July-August); (d) the amount of precipitation during previous October-current
 176 April (snow) and current May-September (rain) shown with blue bars, in August and whole summer period JJA (June-July-



177 August) shown with triangles and circles. Both the mean NDVI of the 10-km plot and the transect decreased from 1999 to 2019
178 (-0.0009 and -0.0010 year⁻¹, respectively), but not with statistically significant trends. Generally, the mean NDVI in the transect
179 was higher than that in the 10-km plot, except for 2000 and 2014.

180 3.2 NDVI of each forest type

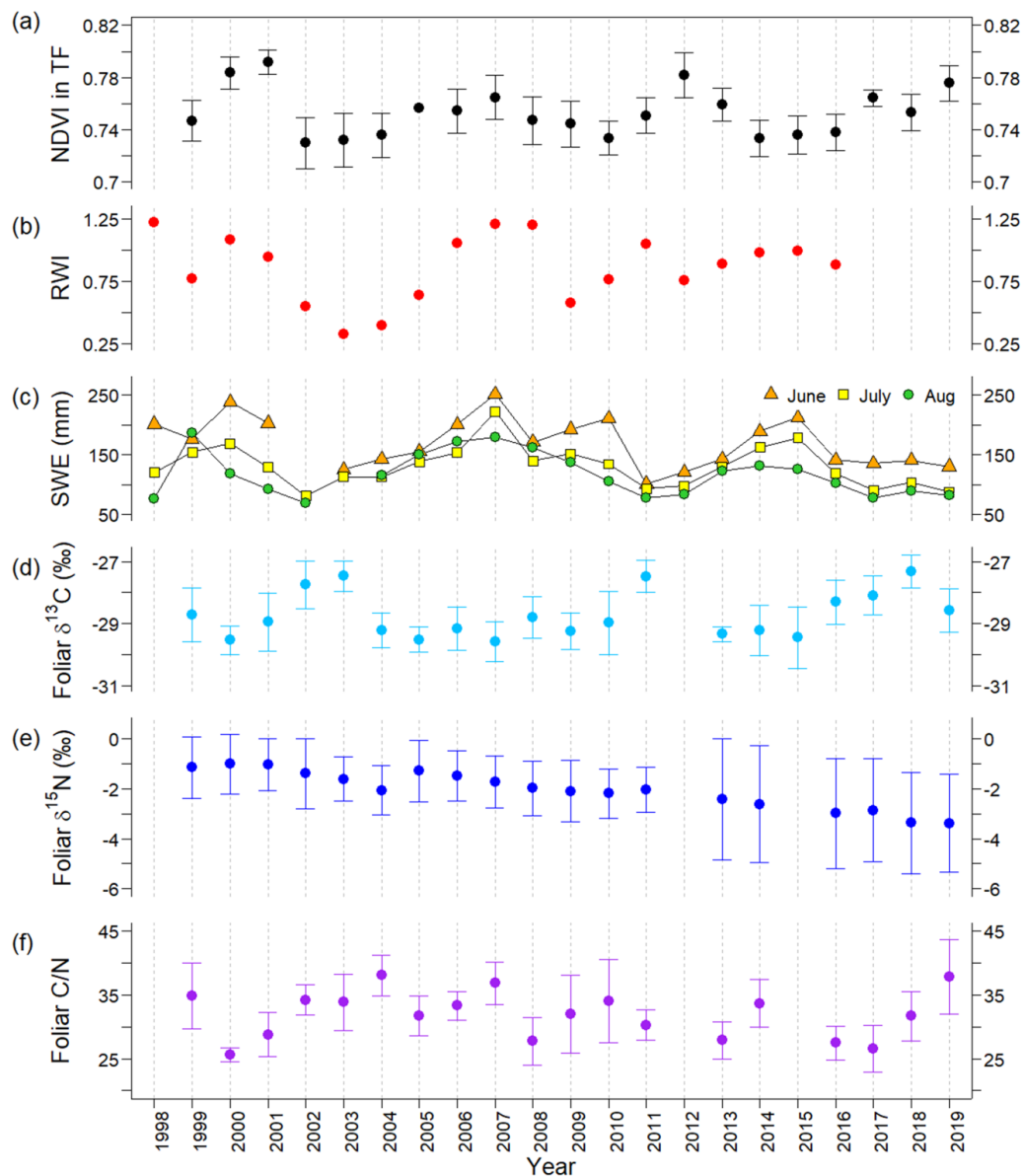
181 The NDVI time series for four forest types (typical forest TF, regenerating forests RF-1 and RF-2, and damaged forest DF) in
182 the transect during 1999–2019 are shown in Fig. 2b. As shown in Fig. 2b and 3a, before 2007, the NDVI of TF during 1999–
183 2001 (0.75 ± 0.02 to 0.79 ± 0.01 , $n = 17$) was higher than that in the subsequent period, 2002–2006 (0.73 ± 0.02 to 0.75 ± 0.02 ,
184 $n = 17$). There was a significant decrease in the TF NDVI between 2002 and 2004 (Fig. 2b and 3a). During 1999–2006, the
185 NDVI values of the four types were close to each other, but after the wet event, NDVI values noticeably differed among the
186 forest types (Fig. 2b). In 2007, the NDVI of TF (0.76 ± 0.02 , $n = 17$) was the highest, and those of the other three types
187 decreased in the order of RF-1 (0.72 ± 0.03 , $n = 11$), RF-2 (0.68 ± 0.02 , $n = 4$), and DF (0.67 ± 0.02 , $n = 2$) (Fig. 2b). In 2008,
188 the NDVI decreased slightly and showed the same order of forest types as that in 2007. After 2009, the difference among the
189 forest types, especially between TF and DF, remained, although it was smaller than that in 2007.

190 3.3 NDVI of the typical forest and ecosystem parameters of the study site

191 To consider the historical variation in the NDVI of typical forests in our study area, the TF NDVI and observed parameters
192 were compared (Fig. 2 and 3). In Fig. 4, the linear relationships between NDVI and other parameters were investigated for two
193 different time periods, before (1999–2006) and after (2008–2019), to compare them.

194 3.3.1 Climate parameters (temperature and precipitation) at Yakutsk

195 Interannual variations in climatic parameters, such as air temperature and precipitation, from 1999 to 2019 are displayed in Fig.
196 2c and 2d. The average air temperature in June–August (summer temperature) was relatively high in 1998, 2001–2002, and
197 2008–2012 (Fig. 2c). TF NDVI did not show any correlation with summer temperature. The amount of annual water
198 precipitation (from October to September) for the period from 1991 to 2020 averaged approximately 233 ± 47 mm. As shown
199 in Fig. 2d, larger water year precipitation, that is, precipitation higher than 280 mm (one standard deviation above the mean for
200 1991–2020), was observed in 2003 (287 mm), 2005–2007 (285, 340, and 296 mm), and 2013 (304 mm). The amount of water
201 precipitation in 2001 (124 mm) was the lowest during the observation period. The drought year (2001) showed a high TF NDVI
202 value. Consecutive wet years in 2005–2007 showed slightly higher TF NDVI values, but there was no correlation between the
203 water year precipitation and NDVI.



204

205

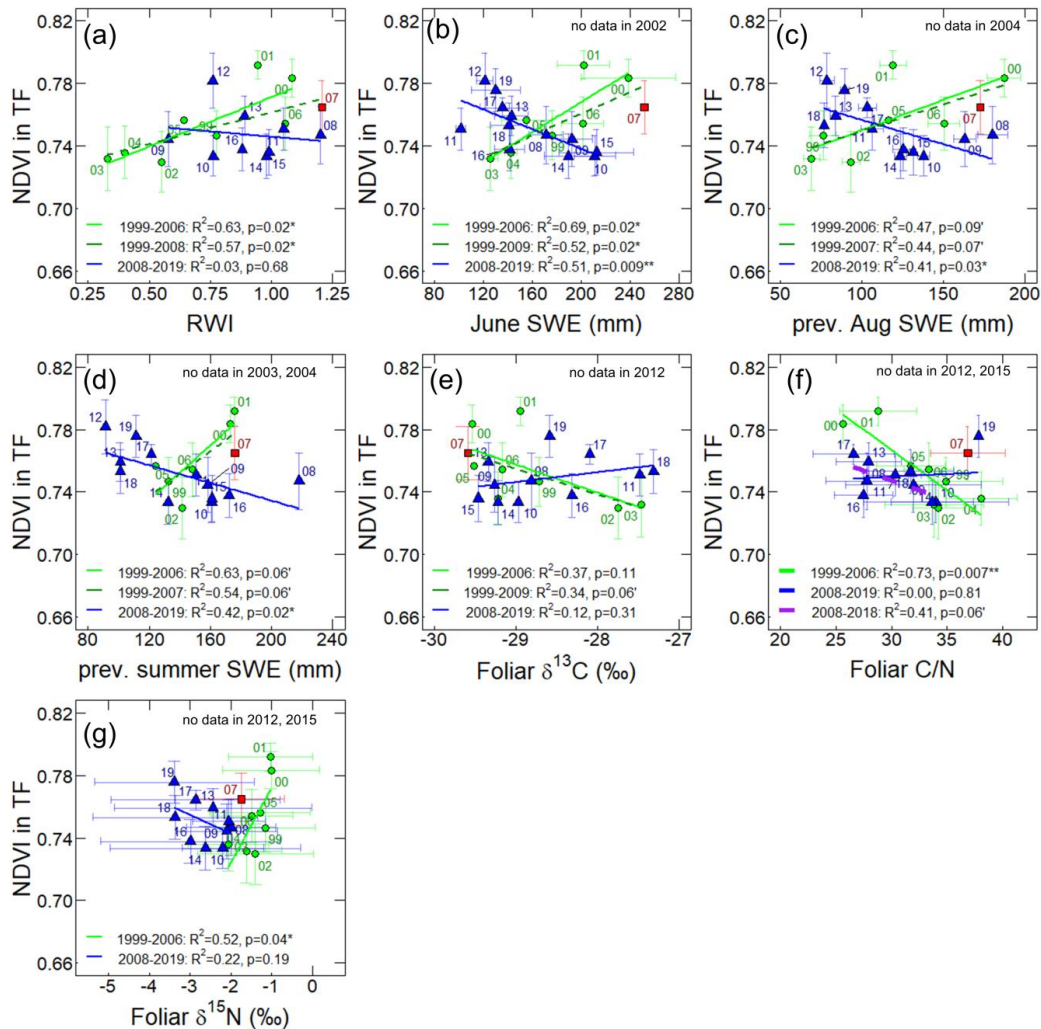
206

207

208

209

Figure 3. The temporal variations in ecosystem parameters observed during 1998–2019 at the typical forest (TF): (a) NDVI, (b) larch ring width index (RWI), (c) soil moisture water equivalent (SWE) at the depth of 0–60 cm in June, July, and August, (d) average foliar $\delta^{13}\text{C}$, (e) $\delta^{15}\text{N}$, and (f) C/N ratio. Error bars represent standard deviations. There were no data for NDVI in 1998, RWI during 2017–2019, June SWE in 2002, August SWE in 2003, foliar $\delta^{13}\text{C}$ in 1998 and 2012, and foliar $\delta^{15}\text{N}$ and C/N in 1998, 2012, and 2015.



210

211 **Figure 4.** The relationships between the TF NDVI in transect and (a) larch RWI during 1999–2016, the monthly average
 212 of SWE (mm) in (b) June and (c) the previous August, (d) averaged monthly SWE for June–August of the previous year,
 213 (e) foliar $\delta^{13}\text{C}$, (f) C/N, and (g) $\delta^{15}\text{N}$ during 1999–2019. The green circles, red square, and blue triangles show data points
 214 during 1999–2006, 2007, and 2008–2019, respectively. Labels nearby the data points are observation years of the TF
 215 NDVI. Horizontal and vertical error bars represent standard deviations. Green and blue solid lines show linear regressions
 216 for 1999–2006 (before the wet event) and 2008–2019 (after the wet event), respectively, and dark green and purple dotted
 217 lines represent other periods. p -values and R^2 describe the significance and the degree of variability of the regression
 218 models, respectively.

219 3.3.2 RWI at the typical forest

220 The larch RWI showed a trend similar to that of the transect TF NDVI during 1999–2007 (Fig. 3a and b). The RWI and average



221 TF NDVI showed high values in 2000–2001 (0.95–1.08 and 0.78–0.79) followed by low values in 2002–2003 (0.33–0.55 and
222 0.73); the RWI in 2003 was the lowest for the whole observation period. Subsequently, both parameters increased by 2007
223 (1.21 and 0.76). After 2007, these two parameters exhibited different behaviors. During the period from 2010 to 2013, a one-
224 year time lag was observed in the TF NDVI: there was an increase in RWI from 2009 to 2011, a decrease in 2012, and one year
225 later, from 2010 to 2012, the TF NDVI increased and then decreased in 2013. Statistically, the temporal correlation between
226 the TF NDVI and RWI was positive at a moderately significant level during 1999–2016 ($r = 0.41$, $p < 0.1$; Table S8), with a
227 significant positive correlation before 2007 ($r = 0.79$, $p < 0.05$; Fig. 4a, Table S6) and an insignificant negative correlation after
228 2007 (Fig. 4a, Table S6).

229 3.3.3 Soil moisture water equivalent at the typical forest

230 The time series of the SWE and TF NDVI showed different correlations in the early and late halves of the observation period
231 (Fig. 3a and 3c). During 1999–2007, the averaged SWE for June–August (hereafter, summer SWE) and the TF NDVI mostly
232 showed similar trends. High values of the TF NDVI in 2000 and 2001 corresponded to high values of the SWE in the current
233 June (239 and 202 mm) and in the last summer (173 and 176 mm in 1999 and 2000). These high values of TF NDVI and SWE
234 were followed by low values during the drought period in 2002–2003. Subsequently, as summer SWE increased from 2004
235 (124 mm) to 2007 (218 mm), the TF NDVI also increased. Therefore, before 2007, the TF NDVI showed the lowest values
236 during the dry years, but the highest values were observed in the wet years (Table 1). For the period from 2008 to 2019, the
237 correlation between the TF NDVI and summer SWE was negative, with a one-year time lag in the SWE (Fig. 3a and 3c). A
238 low summer SWE value was observed in 2011 (91 mm), and a high TF NDVI value was observed in the subsequent year, 2012.
239 After 2016, the TF NDVI showed an increasing trend, whereas the SWE decreased from 2015 to 2019. Statistically, the TF
240 NDVI showed positive correlations with the SWE in the current June ($r = 0.83$, $p < 0.05$) and the previous summer ($r = 0.79$,
241 $p < 0.1$), including the previous July ($r = 0.82$, $p < 0.05$) and previous August ($r = 0.69$, $p < 0.1$), during the period from 1999
242 to 2006 (Fig. 4b–d and S4d; Table S6). However, after 2008, TF NDVI showed negative correlations with the SWE in the
243 previous ($r = -0.65$, $p < 0.05$) and current ($r = -0.73$, $p < 0.01$) summer, at a stronger significance level (Fig. 4b–d and S4a–e;
244 Table S6). During and after 2007, there was no change in the TF NDVI; slightly damaged RF-1 showed a decrease in NDVI
245 to levels similar to those observed during the 2002 drought (Table 1).

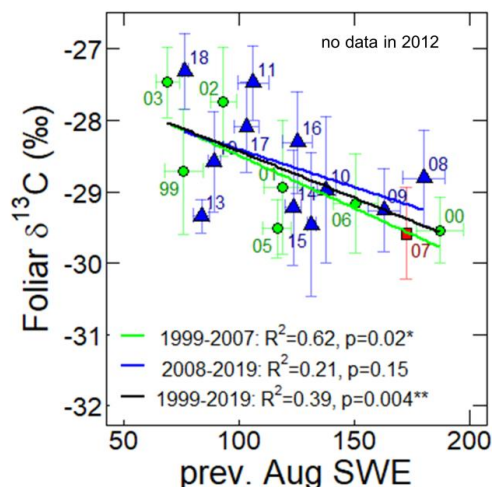


246 **Table 1.** Mean and standard deviation of seasonal maximum NDVI of all plots in the TF and RF-1 in the periods before (1999–
 247 2006), during (2007), and after (2008–2019) the extreme wet event. Averaged NDVI was also calculated for wet and dry periods
 248 before the event. Different letters in the superscript (a, b, c, and d) indicate a statistical difference between the means, calculated
 249 using either the Student’s *t*-test, Welch *t*-test, or Wilcoxon rank-sum test. The sample size (*n*) indicates the number of plots in
 250 an NDVI data group.

Forest type	before the wet event			during the wet event (2007)	after the wet event (2008-2019)
	wet period (2000, 2001, 2006)	dry period (2002)	1999-2006		
Typical	0.78±0.02 ^a (n=54)	0.73±0.02 ^b (n=17)	0.75±0.03 ^{c,d} (n=120)	0.76±0.02 ^c (n=17)	0.75±0.02 ^d (n=182)
Regenerating-1	0.79±0.03 ^a (n=33)	0.73±0.02 ^b (n=11)	0.76±0.03 ^c (n=86)	0.72±0.03 ^b (n=11)	0.74±0.03 ^b (n=115)

251 **3.3.4 Larch needle $\delta^{13}\text{C}$, $\delta^{15}\text{N}$, C/N at the typical forest**

252 As shown in Fig. 3a and 3d, the foliar $\delta^{13}\text{C}$ and TF NDVI moved in opposite directions in the early half of the observation
 253 period (from 1999 to 2009) (Fig. 3a and 3d). For example, in 2000 and 2001, the TF NDVI had large values, while the foliar
 254 $\delta^{13}\text{C}$ values were low (-29.5 ± 0.5 and $-28.9 \pm 0.9\%$). During the period from 2002 to 2007, TF NDVI increased, and at the
 255 same time, foliar $\delta^{13}\text{C}$ values decreased. Foliar $\delta^{13}\text{C}$ values higher than -28.0% were observed in 2002, 2003, 2011, and 2018,
 256 when low summer SWE and TF NDVI were observed (Fig. 3a and 3d). The correlation between foliar $\delta^{13}\text{C}$ and TF NDVI was
 257 statistically insignificant without a time lag (Fig. 3e, Tables S6–8), but there was a significant correlation between foliar $\delta^{13}\text{C}$
 258 and TF NDVI with a time lag of foliar $\delta^{13}\text{C}$ after the wet event (Table S7). Foliar $\delta^{13}\text{C}$ was negatively correlated with the
 259 previous August SWE during 1999–2007 ($r = -0.79$, $p < 0.05$) and 1999–2019 ($r = -0.62$, $p < 0.01$) (Fig. 5), but also with the
 260 SWE in the current year June and July for the period from 1999 to 2007, and June to August for 2008 to 2019 (Table S9).
 261 Similar to $\delta^{13}\text{C}$, foliar C/N and TF NDVI moved in opposite directions (Fig. 3a and 3f). In 2000 and 2001, the foliar C/N had
 262 low values (25.6 ± 1.1 and 28.8 ± 3.4 , respectively), while the TF NDVI was high. There was also a distinct negative correlation
 263 between trends in C/N and TF NDVI before and after 2007, excluding 2019 (Fig. 4f).
 264 Foliar $\delta^{15}\text{N}$ values decreased after 2005 (Figure 3e). A positive correlation was observed between foliar $\delta^{15}\text{N}$ and TF NDVI
 265 before 2007 (Fig. 3a, 3f, and 4g).
 266



267 **Figure 5.** The relationship between the foliar $\delta^{13}\text{C}$ and monthly mean SWE in the previous August (mm) during 1999–2019.
 268 The green circles, red square, and blue triangles show data points during 1999–2006, 2007, and 2008–2019, respectively.
 269 Labels nearby the data points are observation years of the foliar $\delta^{13}\text{C}$. Vertical error bars represent standard deviations. The
 270 linear regressions for 1999–2007, 2008–2019, and 1999–2019 are presented by green, blue, and black solid lines. p -values and
 271 R^2 describe the significance and the degree of variability of the regression models, respectively.

272 4 Discussion

273 4.1 NDVI variation among forest conditions

274 Before 2007, there was a small difference in the NDVI among the four forest types (Fig. 2b and Table S5). In most years before
 275 2007, the NDVI values in RF and DF were higher than those in TF. During 2007–2008, there was a large difference in NDVI
 276 among the forest types, especially between the TF and DF (Fig. 2a). During this period, the SWE reached extremely high
 277 values (Fig. 3c), caused by a large precipitation amount during 2005–2008 (Fig. 2d). Consequently, the forest floor was partially
 278 waterlogged, resulting in damage to the larch forest, especially in the DF and RF transects. These data indicate that during the
 279 drought years (before 2007), wet sites such as DF and RF showed higher NDVI values than dry TF sites because of higher
 280 water availability. However, after 2007, the TF, which was visually unaffected by the wet event, showed a higher NDVI than
 281 the DF and RF. The presence of surface water in DF and soil saturated with water in DF and RF could also reduce the NDVI
 282 values.

283 After 2009, as the soil became dry, the difference in NDVI among the forest types decreased (Fig. 2b). This may have been
 284 caused by the change in the vegetation in RF and DF, that is, the change from mature larch trees to understory and floor
 285 vegetation, such as water-tolerant species and seedlings of birch and larch trees via secondary succession. In 2016, the
 286 difference in NDVI between TF and DF increased again (Fig. 2b). This may have been caused by the high SWE observed in



287 2015 (Fig. 3c), which lowered the NDVI in RF and DF.

288 However, the difference in NDVI between TF and DF remained at the end of the observation period. Previously, the spatial
289 variation in NDVI along the transect was investigated a decade after the wet event in 2018 (Nogovitycyn et al., 2022).
290 Nogovitycyn et al. (2022) concluded that NDVI was higher in TF than in DF because of a difference in the stand density of
291 mature trees, as NDVI indicates a leaf area index (LAI), which corresponds to the number of mature trees in this forest.

292 4.2 Trends in NDVI of the transect and 10-km plot

293 The NDVI of the 10-km plot showed a trend similar to that of the transect NDVI during the observation period ($r = 0.78$, $p <$
294 0.001), as shown in Fig. 2a, and the mean NDVI value of the 10-km plot was lower than that of the transect in most years. We
295 found year-to-year variations in both NDVI datasets, but no significant increasing or decreasing trends were observed, which
296 is consistent with the observations during previous studies at this site (Nagano et al., 2022; Tei et al., 2019b; Lloyd et al., 2011).
297 Therefore, our observational data can be used for the analyses of ecosystem changes not only at the plot scale but also at the
298 regional scale.

299 4.3 Historical variation in NDVI of typical forest

300 We studied historical variations in NDVI and field-observed ecosystem and climatic parameters of a typical forest to understand
301 forest conditions.

302 4.3.1 Water availability

303 As described in the Sect. 3.3.3, SWE controls forest NDVI because the observation site (northeastern taiga) is established in a
304 continental dry area. We found positive and negative correlations between the NDVI and SWE. Before 2007, the TF NDVI
305 was positively correlated with the June SWE in the current year (Fig. 4b) and positively correlated with the SWE in the previous
306 year June, July, August, and the previous year summer (JJA: June–July–August) (Fig. 4c, 4d, S4c, and S4d, Table S6). This
307 indicates the influence of hydrological conditions in the previous year and early summer of the current year on the leaf
308 productivity of larch trees in the current year.

309 Larches, as deciduous trees, assimilate carbon through photosynthesis (photoassimilate) during the summer to prepare needles
310 in the next year, and the elongation of needles may be affected by hydrological conditions in the early summer. In the Spasskaya
311 Pad Forest, pulse-labeling experiments with $^{13}\text{CO}_2$ showed that stored carbon from the previous year contributed approximately
312 50 % to formation of new needles in *Larix gmelini* saplings (Kagawa et al., 2006). The high level of water availability in the
313 summers of 1999 and 2000 contributed to increased carbon storage and, as a result, the high formation of needles in 2000 and
314 2001. The significant NDVI decrease in 2002 was caused by a low level of soil moisture (i.e., dry conditions). The high summer
315 air temperature (Fig. 2c) and the small amount of precipitation (Fig. 2d) in 2001 and 2002 caused droughts in 2002 and 2003.



316 Subsequently, the soil moisture increased due to a large amount of water year precipitation (Fig. 2d), which contributed to an
317 increase in NDVI until 2007.

318 It is known that the NDVI depends on the previous-year precipitation in arid and semi-arid regions (e.g., Burry et al., 2018;
319 Camberlin et al., 2007). In addition, historical time series of climate indices, based on both precipitation and temperature, were
320 related to one-year lagged NDVI (e.g., Verbyla, 2015; Liu et al., 2017). In boreal interior Alaska, the summer moisture index
321 showed a correlation with maximum summer NDVI not only at a one-year time lag in two 10-km climate station buffers but
322 also at a two-year time lag in many other ones (Verbyla, 2015). Possible reasons for the multi-year NDVI lag could be the long-
323 term negative vegetation responses to drought events, such as a decrease in carbon allocation by plants (e.g., Kannenberg et
324 al., 2019) and plant mortality (e.g., Anderegg et al., 2012). Negative effects of drought events also occurred in our study (Table
325 1).

326 The effect of the preceding hydrological conditions on NDVI is also evidenced by the significant negative correlation between
327 foliar $\delta^{13}\text{C}$ and the previous August SWE during 1999–2007 ($r = -0.79$, $p < 0.05$; Fig. 5). The mechanism by which plant $\delta^{13}\text{C}$
328 responds to changes in light and water availability has been well explained in previous studies (e.g., Farquhar et al., 1989).
329 Under drought stress during 2001–2002, there was a decrease in needle stomatal conductance, resulting in a decrease in carbon
330 assimilation. In the subsequent years, 2002–2003, larches produced fewer needles (lower NDVI) from the previously
331 photosynthesized carbon, and as a result, had high $\delta^{13}\text{C}$ values. Comparing the decrease in TF NDVI for drought events, the
332 decrease in TF NDVI for the extreme wet event was not as large (Fig. 2b and 3a), although the extreme wet event caused a
333 significant decrease in the NDVI of RF-1 and RF-2. However, the positive correlations between the TF NDVI and soil moisture,
334 observed during 1999–2006, shifted to negative correlations during 2008–2019 (Fig. 4b–d and S4a–e). After 2007, the TF
335 NDVI was negatively correlated with the SWE of all months in the previous (with a one-year time lag) and current years
336 (without a lag) (Table S6). This may indicate that after the extreme wet event, the soil moisture in the previous and current
337 years seemed to negatively affect the current TF NDVI. Therefore, a high level of soil moisture may affect needle production
338 (i.e., carbon assimilation, needle formation, and/or needle elongation). However, based on the foliar $\delta^{13}\text{C}$ data, there was no
339 evidence that the needle stomatal conductance, which is an indicator of the rates of transpiration and carbon assimilation, was
340 disturbed by the event because the correlation between foliar $\delta^{13}\text{C}$ and SWE remained negative during 2008–2019, similar to
341 that during 1999–2007 (Table S9). During 2008–2019, foliar $\delta^{13}\text{C}$ was mainly controlled by hydrological conditions in the
342 current year rather than those in the previous year. In years with a high SWE, such as 2009 and 2015, stomatal conductance
343 increased (low foliar $\delta^{13}\text{C}$), which usually indicates the higher potential of a plant to assimilate CO_2 , store C, and produce
344 needles (high TF NDVI) in the current and subsequent years. Nevertheless, in these wet years and in the subsequent years of
345 2010 and 2016, the TF NDVI values were low. Therefore, the decrease in the TF NDVI in wet years may be due to factors
346 other than the carbon assimilation process. Nitrogen availability for larches can control needle formation at the beginning of



347 the growing season and their elongation, and consequently, the TF NDVI.

348 **4.3.2 Nitrogen availability**

349 Before 2007, the TF NDVI showed a significant negative correlation with foliar C/N (Fig. 4f), indicating a positive correlation
350 with foliar N content. In this ecosystem, there have been no previous studies on the temporal correlation between NDVI and
351 plant N content (or $\delta^{15}\text{N}$). Changes in leaf nitrogen, which is an important element of chlorophyll (green pigment), were
352 detected using NDVI (Gamon et al., 1995). Previously, the relationship between NDVI and leaf N content was predominantly
353 investigated in crops for agricultural purposes but not in natural ecosystems. In coniferous forests, the estimation of foliar
354 nitrogen using remote-sensing methods showed the highest uncertainty due to the complex structure of needleleaf canopies
355 (reviewed by Homolova et al., 2013).

356 As leaf N content is considered to be an indicator of nitrogen availability for a plant in some boreal regions, where the ecosystem
357 is usually poor in N (Matsushima et al., 2012; Liang et al., 2014), we concluded that forest greenness (NDVI) was strongly
358 controlled by nitrogen uptake by larch trees. Therefore, soil moisture is suggested to play a crucial role in maintaining forest
359 nitrogen status. During 2000–2001, soil water was available for plants and induced favorable conditions for soil nitrogen uptake
360 by trees. Under suitable soil moisture conditions, the production of soil inorganic N may increase. This may lead to a high
361 production of larch needles (high NDVI). During 2002–2003—the drought years—dry conditions caused less productivity of
362 soil inorganic N and less N uptake by trees. In the post-drought period of 2004–2007, an increase in soil moisture gradually
363 recovered the forest conditions in terms of nitrogen uptake and needle production.

364 After 2007, the foliar C/N still showed a negative correlation with the TF NDVI during 2008–2018, but this correlation was
365 statistically weaker compared to that during 1999–2006 (Fig. 4f). At the same time, the positive correlations between the TF
366 NDVI and SWE changed to negative ones during 2008–2019. According to these results, high soil moisture could lead to low
367 needle production under low nitrogen availability. When extremely high soil moisture, resulting in the saturation of soil with
368 water, caused less production of soil inorganic nitrogen, low TF NDVI and high C/N values may be observed; thus TF NDVI
369 and SWE were negatively correlated.

370 While N content reflects the plant's nitrogen status, plant $\delta^{15}\text{N}$ is widely accepted to depend on the isotopic composition of
371 nitrogen sources (e.g., Evans, 2001). Therefore, the $\delta^{15}\text{N}$ of soil inorganic ammonium NH_4^+ , which is the main nitrogen source
372 in the Spasskaya Pad forest (Popova et al., 2013), presumably determined the foliar $\delta^{15}\text{N}$ in larches. As shown in Fig. 3e, foliar
373 $\delta^{15}\text{N}$ gradually decreased after 2005. These data suggest that larch trees used less soil inorganic N, especially from the deeper
374 soil layers, which usually have higher soil $\delta^{15}\text{N}$. This may be related to either a change in soil N dynamics, a decrease in the
375 vertical distribution of roots (Takenaka et al., 2016), or damage to the lower roots due to extremely high soil moisture. Under
376 root oxygen stress due to soil flooding, plant metabolism changes from aerobic respiration to anaerobic fermentation,
377 characterized by energy deficiency and ethanol production, both of which induce decreased nutrient uptake and plant growth



378 (reviewed by Pezeshki and Delaune, 2012). Reduced soil conditions can also induce soil phytotoxin production, damaging the
379 root system (Pezeshki, 2001).

380 It should be noted that not only the extreme wet event in 2007, but also the extreme drought in 2001 may have caused a change
381 in N availability. Many studies have shown that foliar $\delta^{15}\text{N}$ increases during drought (Penuelas et al., 2000; Handley et al.,
382 1999; Lopes and Araus, 2006; Ogaya and Penuelas, 2008). However, in the present study, the drought in 2001 and 2002
383 decreased foliar $\delta^{15}\text{N}$. We could not identify the exact reason, but drought in 2001 and 2002 might have affected the N
384 availability for larch trees.

385 **4.3.3 NDVI and RWI of larch trees**

386 Two parameters of aboveground biomass, the RWI and TF NDVI, were positively correlated at a significant level ($r = 0.79$, p
387 < 0.05 ; Fig. 4a) during 1999–2006. Similarly, in other northern regions, temporal patterns of the NDVI and dendrochronological
388 data were similar for larch (Erasmí et al., 2021; Berner et al., 2011; Berner et al., 2013), pine (Berner et al., 2011), and spruce
389 (Andreu-Hayles et al., 2011; Beck et al., 2013; Berner et al., 2011; Lopatin et al., 2006). This means that tree growth (RWI)
390 and needle production (NDVI as an indicator of LAI) showed synchronous responses to environmental changes before 2007.
391 However, there was no significant correlation between the TF NDVI and RWI after 2007. Thus, the extreme wet event in 2007
392 could have changed the physiological response of larch trees to the environment in terms of needle and wood production.

393 The correlation between NDVI and RWI at our observation site was previously reported by Tei et al. (2019b). They used
394 GIMMS-NDVI3g and found its positive correlation with the RWI in the subsequent year during 2004–2014 at the study site.
395 These two parameters, the NDVI and RWI, reflect the carry-over of carbon, which is fixed via needles in the previous year and
396 used in the current year, as experimentally demonstrated by Kagawa et al. (2006). In our study, we could not find a significant
397 correlation between the TF NDVI and RWI at the one-year lag of RWI (Fig. S4g). In previous studies, dendrochronological
398 data showed that tree growth responded to climate with a time lag (e.g., Tei and Sugimoto, 2018). In our study, soil moisture
399 and nitrogen availability for trees seemed to be the key factors of the environment affecting not only the NDVI, as mentioned
400 above, but also the RWI. However, the TF NDVI and RWI were not significantly correlated after 2007, whereas there was a
401 significant positive correlation before 2007. Thus, the extreme wet event in 2007 could have changed the physiological
402 response of larch trees to the environment in terms of needle and wood production.

403 **4.4 Changes in larch forest NDVI due to drought and the extreme wet event**

404 As shown in Fig. 2b, the NDVI in TF showed a significant decrease in 2002. Such a decrease in NDVI has been repeated in
405 the past because the climate is continental (dry) in this region. Compared to this decrease in NDVI due to drought, the extreme
406 wet event in 2007 showed only a slight decrease in the NDVI in TF, although the NDVI in DF and RF-2 decreased considerably.
407 Tree mortality in the DF and RF during the extreme wet event is controlled by soil properties and topographic features, that is,



408 depressions (Iwasaki et al., 2010). However, the effects of the event may not only include tree mortality but also invisible
409 damage to living trees. In this study, NDVI, a potential indicator of needle production in a typical forest, was negatively related
410 to the summer SWE in the previous and current years during 2008–2019 and with the current-year needle C/N during 2008–
411 2018 (Table S6). This may indicate that needle production in the current and subsequent years during the summer was disturbed
412 by increased soil moisture and decreased soil N uptake by trees. We suggest that N uptake by larches might be reduced in wet
413 soils due to damaged lower roots, decreased vertical distribution of roots (Takenaka et al., 2016), or altered soil N production.
414 Changes in the process of needle production may affect tree growth in the current and subsequent years in the forest (Kagawa
415 et al., 2006; Tei et al., 2019b). However, we found no evidence that tree radial growth was disturbed after 2007, and the RWI
416 responded well to changes in the SWE (Fig. 3b and 3c). Additionally, at the ecosystem scale, there was no significant change
417 in the CO₂ exchange measured by the 32-m flux tower in this larch forest (Kotani et al., 2019). However, the observed increase
418 in understory biomass was suggested to compensate for negative changes in fluxes at the overstory level (Kotani et al., 2019)
419 and in the NDVI of the forest (Nagano et al., 2022). This means that the negative effects of the extreme wet event on living
420 larch trees were not excluded in the previous studies. Our study showed that limitation in N uptake at high soil moisture levels
421 is one of the factors that may potentially reduce tree growth in the future.

422 In our previous study (Nogoviteyn et al., 2022), spatial variations in NDVI and foliar traits identified favorable conditions in
423 the sites affected by the extreme wet event (RF). The larch forest in RF with lower NDVI (lower stand density) had higher
424 light (higher $\delta^{13}\text{C}$) and nitrogen (lower foliar C/N) availability for one mature larch tree than that in unaffected areas (TF)
425 because of reduced competition for light and soil nitrogen among trees. Such favorable conditions and the presence of a large
426 number of young larch trees may lead to further RF succession after an extremely wet event. However, because weather
427 extremes are expected to be more frequent and intensive, the period between extremes may exceed the period of recovery after
428 the extremes. Therefore, in the future, forests may be damaged rather than recovered. Regarding the prediction of tree growth
429 in this dry region, there is a discrepancy between the different vegetation models. In eastern Siberia, the dynamic global
430 vegetation model (DGVM) simulated increased forest production in the nearest century, whereas the RWI-based model showed
431 the opposite result (Tei et al., 2017). Some models may overestimate production because they do not include important
432 parameters such as soil moisture, soil N production, and N uptake by trees. To better understand changes in the forest, long-
433 term observation of variations in soil N availability depending on soil moisture and other factors is necessary.

434 **5 Conclusions**

435 In this study, historical variations in satellite-derived NDVI (forest greenness) and field-observed parameters of larch forests
436 were investigated to understand the effects of the extreme wet event on the larch forests of northeastern Siberia. The NDVI
437 values of the plots visually unaffected (typical mature larch forest, TF) and affected by the event were similar before 2007 but



438 differed after 2007 because of the high tree mortality caused by waterlogging and the presence of water in the depression.
439 Although the TF was visually unaffected by the event, it also underwent changes. Temporal correlations revealed that before
440 the wet event, needle production (TF NDVI) was positively related to the SWE in the previous summer and current June and
441 tree-ring growth (RWI). In this dry region, larches used the previous-year soil water to make photosynthates (carbon assimilated
442 by photosynthesis) to prepare needles and wood in the current year and used the early summer soil water for the elongation of
443 needles in the current year. In addition, the TF NDVI showed significant negative correlations with needle C/N ratio (or positive
444 correlation with needle N content) before the wet event, and this correlation continued until 2018 (except for 2007). This
445 indicates that nitrogen is an important parameter for this ecosystem before and after a wet event. The $\delta^{15}\text{N}$ in 1999-2006 showed
446 a positive correlation with TF NDVI. Under suitable soil moisture conditions, the production of soil inorganic N, and
447 consequently, the production of larch needles, may be increased. However, after the wet event in 2008-2019, the temporal
448 correlations between the TF NDVI and SWE in the previous summer and current June surprisingly shifted from positive to
449 negative. Needle N content was positively correlated with the TF NDVI and negatively correlated with the SWE in June. In
450 addition, needle $\delta^{15}\text{N}$ generally decreased, indicating that larches used less inorganic nitrogen from deeper soils, which usually
451 have higher $\delta^{15}\text{N}$. During this period, extremely high soil moisture may have caused inactive soil inorganic N, anaerobic-stress-
452 induced root damage, and/or production of soil phytotoxins, which decreased nitrogen uptake and plant growth.

453 **Data availability.** Yakutsk air temperature and precipitation data are available from the RIHMI-WDC website ([http://aisori-](http://aisori-m.meteo.ru/)
454 [m.meteo.ru/](http://aisori-m.meteo.ru/)). The seasonal maximum NDVI data and larch RWI data are described in the Supplement (Table S1 and S2).
455 All other data (historical records of SWE, and foliar C and N isotopes and contents) presented in this work will be shared
456 upon request and will be deposited in the Arctic Data Archive System (ADS).

457 **Author contributions.** AS designed the research and AN calculated the NDVI and performed the analyses. TM, ST, and NS
458 helped with the analyses, and TCM managed all the field observations. RS and YM helped with field observations. AN and
459 AS prepared the paper with contributions from all co-authors.

460 **Competing interests.** The authors declare that they have no conflict of interest.

461 **Acknowledgements.** The authors are grateful to Dr. A. Kononov, R. Petrov, and other colleagues from the IBPC for
462 supporting our fieldwork at the Spasskaya Pad Forest Station and M. Grigorev for his assistance in the fieldwork. The
463 authors also appreciate Y. Hoshino, S. Nunohashi, A. Alekseeva, and E. Starostin for their support in laboratory work and
464 logistics.



465 **Financial support.** This work was supported by the Belmont Forum Arctic program COPERA (C budget of ecosystems, cities,
466 and villages on permafrost in the eastern Russian Arctic) project, the International Priority Graduate Programs (IPGP), funded
467 by the Ministry of Education, Culture, Sports, Science, and Technology-Japan (MEXT), and the Hokkaido University DX
468 Doctoral Fellowship (Grant No. JPMJSP2119), funded by the Japan Science and Technology Agency.

469 **References**

- 470 Abaimov, A. P., Lesinski, J. A., Martinsson, O., and Milyutin, L. I.: Variability and ecology of Siberian larch species, Swedish
471 University of Agricultural Sciences. Department of Silviculture. Reports., Umeå, 123 pp., 1998.
- 472 Anderegg, W. R. L., Berry, J. A., Smith, D. D., Sperry, J. S., Anderegg, L. D. L., and Field, C. B.: The roles of hydraulic and
473 carbon stress in a widespread climate-induced forest die-off, *Proceedings of the National Academy of Sciences of the United*
474 *States of America*, 109, 233-237, 10.1073/pnas.1107891109, 2012.
- 475 Andreu-Hayles, L., D'Arrigo, R., Anchukaitis, K. J., Beck, P. S. A., Frank, D., and Goetz, S.: Varying boreal forest response to
476 Arctic environmental change at the Firth River, Alaska, *Environmental Research Letters*, 6, 10.1088/1748-9326/6/4/045503,
477 2011.
- 478 Archibold, O. W.: The coniferous forests, in: *Ecology of World Vegetation*, 238–279, 10.1007/978-94-011-0009-0_8 1995.
- 479 Beck, P. S. A., Andreu-Hayles, L., D'Arrigo, R., Anchukaitis, K. J., Tucker, C. J., Pinzon, J. E., and Goetz, S. J.: A large-scale
480 coherent signal of canopy status in maximum latewood density of tree rings at arctic treeline in North America, *Global and*
481 *Planetary Change*, 100, 109-118, 10.1016/j.gloplacha.2012.10.005, 2013.
- 482 Berner, L. T., Beck, P. S. A., Bunn, A. G., and Goetz, S. J.: Plant response to climate change along the forest-tundra ecotone in
483 northeastern Siberia, *Global Change Biology*, 19, 3449-3462, 10.1111/gcb.12304, 2013.
- 484 Berner, L. T., Beck, P. S. A., Bunn, A. G., Lloyd, A. H., and Goetz, S. J.: High-latitude tree growth and satellite vegetation
485 indices: Correlations and trends in Russia and Canada (1982-2008), *Journal of Geophysical Research-Biogeosciences*, 116,
486 10.1029/2010jg001475, 2011.
- 487 Burry, L. S., Palacio, P. I., Somoza, M., de Mandri, M. E. T., Lindsoug, H. B., Marconetto, M. B., and D'Antoni, H. L.:
488 Dynamics of fire, precipitation, vegetation and NDVI in dry forest environments in NW Argentina. *Contributions to*
489 *environmental archaeology, Journal of Archaeological Science-Reports*, 18, 747-757, 10.1016/j.jasrep.2017.05.019, 2018.
- 490 Camberlin, P., Martiny, N., Philippon, N., and Richard, Y.: Determinants of the interannual relationships between remote sensed
491 photosynthetic activity and rainfall in tropical Africa, *Remote Sensing of Environment*, 106, 199-216,
492 10.1016/j.rse.2006.08.009, 2007.
- 493 Douville, H., Raghavan, K., Renwick, J., Allan, R. P., Arias, P. A., Barlow, M., Cerezo-Mota, R., Cherchi, A., Gan, T. Y., Gergis,
494 J., Jiang, D., Khan, A., Pokam Mba, W., Rosenfeld, D., Tierney, J., and Zolina, O.: Water Cycle Changes, in: *Climate Change*
495 *2021: The Physical Science Basis. Contribution of Working Group I to the Sixth Assessment Report of the*
496 *Intergovernmental Panel on Climate Change* edited by: Masson-Delmotte, V., Zhai, P., Pirani, A., Connors, S. L., Péan, C.,
497 Berger, S., Caud, N., Chen, Y., Goldfarb, L., Gomis, M. I., Huang, M., Leitzell, K., Lonnoy, E., Matthews, J. B. R., Maycock,
498 T. K., Waterfield, T., Yelekçi, O., Yu, R., and Zhou, B., Cambridge University Press, Cambridge, United Kingdom and New



- 499 York 1055–1210, 10.1017/9781009157896.010. , 2021.
- 500 Erasmí, S., Klinge, M., Dulamsuren, C., Schneider, F., and Hauck, M.: Modelling the productivity of Siberian larch forests
501 from Landsat NDVI time series in fragmented forest stands of the Mongolian forest-steppe, *Environmental Monitoring and*
502 *Assessment*, 193, 10.1007/s10661-021-08996-1, 2021.
- 503 Evans, R. D.: Physiological mechanisms influencing plant nitrogen isotope composition, *Trends in Plant Science*, 6, 121-126,
504 10.1016/s1360-1385(01)01889-1, 2001.
- 505 FAO: Global Forest Resources Assessment 2020 – Key findings, Rome, 10.4060/ca8753en, 2020.
- 506 Farquhar, G. D., Ehleringer, J. R., and Hubick, K. T.: Carbon isotope discrimination and photosynthesis, *Annual Review of*
507 *Plant Physiology and Plant Molecular Biology*, 40, 503-537, 10.1146/annurev.pp.40.060189.002443, 1989.
- 508 Friedlingstein, P., Jones, M. W., O'Sullivan, M., Andrew, R. M., Bakker, D. C. E., Hauck, J., Le Quere, C., Peters, G. P., Peters,
509 W., Pongratz, J., Sitch, S., Canadell, J. G., Ciais, P., Jackson, R. B., Alin, S. R., Anthoni, P., Bates, N. R., Becker, M., Bellouin,
510 N., Bopp, L., Chau, T. T. T., Chevallier, F., Chini, L. P., Cronin, M., Currie, K. I., Decharme, B., Djeutchouang, L. M., Dou, X.
511 Y., Evans, W., Feely, R. A., Feng, L., Gasser, T., Gilfillan, D., Gkritzalis, T., Grassi, G., Gregor, L., Gruber, N., Gurses, O.,
512 Harris, I., Houghton, R. A., Hurtt, G. C., Iida, Y., Ilyina, T., Luijkx, I. T., Jain, A., Jones, S. D., Kato, E., Kennedy, D., Goldewijk,
513 K. K., Knauer, J., Korsbakken, J. I., Kortzinger, A., Landschutzer, P., Lauvset, S. K., Lefevre, N., Lienert, S., Liu, J. J., Marland,
514 G., McGuire, P. C., Melton, J. R., Munro, D. R., Nabel, J., Nakaoka, S. I., Niwa, Y., Ono, T., Pierrot, D., Poulter, B., Rehder,
515 G., Resplandy, L., Robertson, E., Rodenbeck, C., Rosan, T. M., Schwinger, J., Schwingshackl, C., Seferian, R., Sutton, A. J.,
516 Sweeney, C., Tanhua, T., Tans, P. P., Tian, H. Q., Tilbrook, B., Tubiello, F., van der Werf, G. R., Vuichard, N., Wada, C.,
517 Wanninkhof, R., Watson, A. J., Willis, D., Wiltshire, A. J., Yuan, W. P., Yue, C., Yue, X., Zaehle, S., and Zeng, J. Y.: Global
518 Carbon Budget 2021, *Earth System Science Data*, 14, 1917-2005, 10.5194/essd-14-1917-2022, 2022.
- 519 Gamon, J. A., Field, C. B., Goulden, M. L., Griffin, K. L., Hartley, A. E., Joel, G., Penuelas, J., and Valentini, R.: Relationships
520 between NDVI, canopy structure, and photosynthesis in 3 Californian vegetation types, *Ecological Applications*, 5, 28-41,
521 10.2307/1942049, 1995.
- 522 Handley, L. L., Azcon, R., Lozano, J. M. R., and Scrimgeour, C. M.: Plant delta N-15 associated with arbuscular mycorrhization,
523 drought and nitrogen deficiency, *Rapid Communications in Mass Spectrometry*, 13, 1320-1324, 1999.
- 524 Homolova, L., Maenovsky, Z., Clevers, J., Garcia-Santos, G., and Schaepman, M. E.: Review of optical-based remote sensing
525 for plant trait mapping, *Ecological Complexity*, 15, 1-16, 10.1016/j.ecocom.2013.06.003, 2013.
- 526 Iijima, Y., Ohta, T., Kotani, A., Fedorov, A. N., Kodama, Y., and Maximov, T. C.: Sap flow changes in relation to permafrost
527 degradation under increasing precipitation in an eastern Siberian larch forest, *Ecohydrology*, 7, 177-187, 10.1002/eco.1366,
528 2014.
- 529 Iwasaki, H., Saito, H., Kuwao, K., Maximov, T. C., and Hasegawa, S.: Forest decline caused by high soil water conditions in
530 a permafrost region, *Hydrology and Earth System Sciences*, 14, 301-307, 10.5194/hess-14-301-2010, 2010.
- 531 Ju, J. C. and Masek, J. G.: The vegetation greenness trend in Canada and US Alaska from 1984-2012 Landsat data, *Remote*
532 *Sensing of Environment*, 176, 1-16, 10.1016/j.rse.2016.01.001, 2016.
- 533 Kagawa, A., Sugimoto, A., and Maximov, T. C.: Seasonal course of translocation, storage and remobilization of C-13 pulse-
534 labeled photoassimilate in naturally growing *Larix gmelinii* saplings, *New Phytologist*, 171, 793-804, 10.1111/j.1469-



- 535 8137.2006.01780.x, 2006.
- 536 Kajimoto, T., Matsuura, Y., Sofronov, M. A., Volokitina, A. V., Mori, S., Osawa, A., and Abaimov, A. P.: Above- and
537 belowground biomass and net primary productivity of a *Larix gmelinii* stand near Tura, central Siberia, *Tree Physiology*, 19,
538 815-822, 1999.
- 539 Kannenberg, S. A., Novick, K. A., Alexander, M. R., Maxwell, J. T., Moore, D. J. P., Phillips, R. P., and Anderegg, W. R. L.:
540 Linking drought legacy effects across scales: From leaves to tree rings to ecosystems, *Global Change Biology*, 25, 2978-2992,
541 10.1111/gcb.14710, 2019.
- 542 Kotani, A., Saito, A., Kononov, A. V., Petrov, R. E., Maximov, T. C., Iijima, Y., and Ohta, T.: Impact of unusually wet permafrost
543 soil on understory vegetation and CO₂ exchange in a larch forest in eastern Siberia, *Agricultural and Forest Meteorology*, 265,
544 295-309, 10.1016/j.agrformet.2018.11.025, 2019.
- 545 Liang, M. C., Sugimoto, A., Tei, S., Bragin, I. V., Takano, S., Morozumi, T., Shingubara, R., Maximov, T. C., Kiyashko, S. I.,
546 Velivetskaya, T. A., and Ignatiev, A. V.: Importance of soil moisture and N availability to larch growth and distribution in the
547 Arctic taiga-tundra boundary ecosystem, northeastern Siberia, *Polar Science*, 8, 327-341, 10.1016/j.polar.2014.07.008, 2014.
- 548 Liu, S. L., Zhang, Y. Q., Cheng, F. Y., Hou, X. Y., and Zhao, S.: Response of Grassland Degradation to Drought at Different
549 Time-Scales in Qinghai Province: Spatio-Temporal Characteristics, Correlation, and Implications, *Remote Sensing*, 9,
550 10.3390/rs9121329, 2017.
- 551 Lloyd, A. H., Bunn, A. G., and Berner, L.: A latitudinal gradient in tree growth response to climate warming in the Siberian
552 taiga, *Global Change Biology*, 17, 1935-1945, 10.1111/j.1365-2486.2010.02360.x, 2011.
- 553 Lopatin, E., Kolstrom, T., and Spiecker, H.: Determination of forest growth trends in Komi Republic (northwestern Russia):
554 combination of tree-ring analysis and remote sensing data, *Boreal Environment Research*, 11, 341-353, 2006.
- 555 Lopes, M. S. and Araus, J. L.: Nitrogen source and water regime effects on durum wheat photosynthesis and stable carbon and
556 nitrogen isotope composition, *Physiologia Plantarum*, 126, 435-445, 10.1111/j.1399-3054.2006.00595.x, 2006.
- 557 Matsushima, M., Choi, W. J., and Chang, S. X.: White spruce foliar delta C-13 and delta N-15 indicate changed soil N
558 availability by understory removal and N fertilization in a 13-year-old boreal plantation, *Plant and Soil*, 361, 375-384,
559 10.1007/s11104-012-1254-z, 2012.
- 560 Nagano, H., Kotani, A., Mizuochi, H., Ichii, K., Kanamori, H., and Hiyama, T.: Contrasting 20-year trends in NDVI at two
561 Siberian larch forests with and without multiyear waterlogging-induced disturbances, *Environmental Research Letters*, 17,
562 10.1088/1748-9326/ac4884, 2022.
- 563 Nakai, T., Hiyama, T., Petrov, R. E., Kotani, A., Ohta, T., and Maximov, T. C.: Application of an open-path eddy covariance
564 methane flux measurement system to a larch forest in eastern Siberia, *Agricultural and Forest Meteorology*, 282,
565 10.1016/j.agrformet.2019.107860, 2020.
- 566 Nogoviteyn, A., Shakhmatov, R., Morozumi, T., Tei, S., Miyamoto, Y., Shin, N., Maximov, T. C., and Sugimoto, A.: Changes
567 in Forest Conditions in a Siberian Larch Forest Induced by an Extreme Wet Event, *Forests*, 13, 10.3390/f13081331, 2022.
- 568 Ogaya, R. and Penuelas, J.: Changes in leaf delta C-13 and delta N-15 for three Mediterranean tree species in relation to soil
569 water availability, *Acta Oecologica-International Journal of Ecology*, 34, 331-338, 10.1016/j.actao.2008.06.005, 2008.
- 570 Ohta, T., Kotani, A., Iijima, Y., Maximov, T. C., Ito, S., Hanamura, M., Kononov, A. V., and Maximov, A. P.: Effects of



- 571 waterlogging on water and carbon dioxide fluxes and environmental variables in a Siberian larch forest, 1998-2011,
572 *Agricultural and Forest Meteorology*, 188, 64-75, 10.1016/j.agrformet.2013.12.012, 2014.
- 573 Penuelas, J., Filella, I., Lloret, F., Pinol, J., and Siscart, D.: Effects of a severe drought on water and nitrogen use by *Quercus*
574 *ilex* and *Phillyrea latifolia*, *Biologia Plantarum*, 43, 47-53, 10.1023/a:1026546828466, 2000.
- 575 Pezeshki, S. R.: Wetland plant responses to soil flooding, *Environmental and Experimental Botany*, 46, 299-312,
576 10.1016/s0098-8472(01)00107-1, 2001.
- 577 Pezeshki, S. R. and DeLaune, R. D.: Soil Oxidation-Reduction in Wetlands and Its Impact on Plant Functioning,
578 10.3390/biology1020196, 2012.
- 579 Popova, A. S., Tokuchi, N., Ohta, N., Ueda, M. U., Osaka, K., Maximov, T. C., and Sugimoto, A.: Nitrogen availability in the
580 taiga forest ecosystem of northeastern Siberia, *Soil Science and Plant Nutrition*, 59, 427-441, 10.1080/00380768.2013.772495,
581 2013.
- 582 Roy, D. P., Kovalskyy, V., Zhang, H. K., Vermote, E. F., Yan, L., Kumar, S. S., and Egorov, A.: Characterization of Landsat-7
583 to Landsat-8 reflective wavelength and normalized difference vegetation index continuity, *Remote Sensing of Environment*,
584 185, 57-70, 10.1016/j.rse.2015.12.024, 2016.
- 585 Schuur, E. A. G., McGuire, A. D., Schadel, C., Grosse, G., Harden, J. W., Hayes, D. J., Hugelius, G., Koven, C. D., Kuhry, P.,
586 Lawrence, D. M., Natali, S. M., Olefeldt, D., Romanovsky, V. E., Schaefer, K., Turetsky, M. R., Treat, C. C., and Vonk, J. E.:
587 Climate change and the permafrost carbon feedback, *Nature*, 520, 171-179, 10.1038/nature14338, 2015.
- 588 Shakhmatov, R., Hashiguchi, S., Maximov, T. C., and Sugimoto, A.: Effects of snow manipulation on larch trees in the taiga
589 forest ecosystem in northeastern Siberia, *Progress in Earth and Planetary Science*, 9, 10.1186/s40645-021-00460-5, 2022.
- 590 Sugimoto, A.: Stable Isotopes of Water in Permafrost Ecosystem, in: *Water-Carbon Dynamics in Eastern Siberia. Ecological*
591 *Studies (Analysis and Synthesis)*, edited by: Ohta, T., Hiyama, T., Iijima, Y., Kotani, A., and Maximov, T., Springer, Singapore,
592 10.1007/978-981-13-6317-7_6, 2019.
- 593 Sugimoto, A., Yanagisawa, N., Naito, D., Fujita, N., and Maximov, T. C.: Importance of permafrost as a source of water for
594 plants in east Siberian taiga, *Ecological Research*, 17, 493-503, 10.1046/j.1440-1703.2002.00506.x, 2002.
- 595 Sugimoto, A., Naito, D., Yanagisawa, N., Ichiyanagi, K., Kurita, N., Kubota, J., Kotake, T., Ohata, T., Maximov, T. C., and
596 Fedorov, A. N.: Characteristics of soil moisture in permafrost observed in East Siberian taiga with stable isotopes of water,
597 *Hydrological Processes*, 17, 1073-1092, 10.1002/hyp.1180, 2003.
- 598 Takata, K., Patra, P. K., Kotani, A., Mori, J., Belikov, D., Ichii, K., Saeki, T., Ohta, T., Saito, K., Ueyama, M., Ito, A., Maksyutov,
599 S., Miyazaki, S., Burke, E. J., Ganshin, A., Iijima, Y., Ise, T., Machiya, H., Maximov, T. C., Niwa, Y., O'ishi, R., Park, H., Sasai,
600 T., Sato, H., Tei, S., Zhuravlev, R., Machida, T., Sugimoto, A., and Aoki, S.: Reconciliation of top-down and bottom-up CO₂
601 fluxes in Siberian larch forest, *Environmental Research Letters*, 12, 10.1088/1748-9326/aa926d, 2017.
- 602 Takenaka, C., Miyahara, M., Ohta, T., and Maximov, T. C.: Response of larch root development to annual changes of water
603 conditions in eastern Siberia, *Polar Science*, 10, 160-166, 10.1016/j.polar.2016.04.012, 2016.
- 604 Tei, S. and Sugimoto, A.: Time lag and negative responses of forest greenness and tree growth to warming over circumboreal
605 forests, *Global Change Biology*, 24, 4225-4237, 10.1111/gcb.14135, 2018.
- 606 Tei, S., Sugimoto, A., Yonenobu, H., Kotani, A., and Maximov, T. C.: Effects of extreme drought and wet events for tree



607 mortality: Insights from tree-ring width and carbon isotope ratio in a Siberian larch forest, *Ecohydrology*, 12, 10.1002/eco.2143,
608 2019a.

609 Tei, S., Sugimoto, A., Yonenobu, H., Yamazaki, T., and Maximov, T. C.: Reconstruction of soil moisture for the past 100 years
610 in eastern Siberia by using delta C-13 of larch tree rings, *Journal of Geophysical Research-Biogeosciences*, 118, 1256-1265,
611 10.1002/jgrg.20110, 2013.

612 Tei, S., Sugimoto, A., Kotani, A., Ohta, T., Morozumi, T., Saito, S., Hashiguchi, S., and Maximov, T.: Strong and stable
613 relationships between tree-ring parameters and forest-level carbon fluxes in a Siberian larch forest, *Polar Science*, 21, 146-157,
614 10.1016/j.polar.2019.02.001, 2019b.

615 Tei, S., Sugimoto, A., Yonenobu, H., Matsuura, Y., Osawa, A., Sato, H., Fujinuma, J., and Maximov, T.: Tree-ring analysis and
616 modeling approaches yield contrary response of circumboreal forest productivity to climate change, *Global Change Biology*,
617 23, 5179-5188, 10.1111/gcb.13780, 2017.

618 Verbyla, D.: Remote sensing of interannual boreal forest NDVI in relation to climatic conditions in interior Alaska,
619 *Environmental Research Letters*, 10, 10.1088/1748-9326/10/12/125016, 2015.

620